Microbiological Research 252 (2021) 126863

Contents lists available at ScienceDirect

Microbiological Research

journal homepage: www.elsevier.com/locate/micres

Breaking bad: Better call gingerol for improving antibiotic susceptibility of *Pseudomonas aeruginosa* by inhibiting multiple quorum sensing pathways

Arpit Shukla [a,b], Paritosh Parmar [a], Baldev Patel [a], Dweipayan Goswami [a], Meenu Saraf [a,*]

[a] Department of Microbiology & Biotechnology, University School of Sciences, Gujarat University, Ahmedabad, 380009, Gujarat, India
[b] Department of Biological Sciences & Biotechnology, Institute of Advanced Research, Gandhinagar, 382426, Gujarat, India

ARTICLE INFO

Keywords:
Antibiotic sensitivity
Biofilm
Computational biology
Phenazine
Molecular dynamics
Rhamnolipid

ABSTRACT

Pseudomonas aeruginosa is recognized as a bacterium with many bullets in its armoury and the Achilles heel of the bacterium is that it exudes several pathways that lead to pathogenicity thereby making the application of the strain cautious since the bacterium is known as a 'superbug' ergo, being resistant to multiple antibiotics. The mechanisms of pathogenicity are mainly driven by quorum sensing (QS), a phenomenon that works on cell-cell communication through classical ligand-receptor interactions. QS-mediated pathways enable control of this organism impossible even with the use of antibiotics. Henceforth, interfering with the QS pathways serves as a new mode of action for futuristic antibiotics to decrease the distress of this microbe. We propose gingerol to interfere with various QS-receptors of *P. aeruginosa* (LasR, PhzR and RhlR) which were deduced using *in silico* approach and validated *in vitro* by assessing its impact on EPS, biofilm, pyocyanin and rhamnolipid of the microbe. Further, gingerol was found to increase the antibacterial potency of the antibiotic when applied in integration with ciprofloxacin. The findings provide an insight about preferring the integrated approach of using QS-inhibitors (QSI) in tandem with antibiotics for holistic strategy in fight against the phenomenon of antibiotic resistance acquired by microbes.

1. Introduction

The genus of *Pseudomonas* is known to harbour several opportunistic pathogens, the first superbug (*P. putida*) resistant to multipotent antibiotics was belonging to this genus. The phenomenon of antibiotic resistance is acquired rapidly through various known mechanisms. It is predicted that in next fifty years, there would only be a handful from the existing plethora of antibiotics that could retain its antibacterial potency. *P. aeruginosa* is one such organism which is widely being studied for unravelling the strategies to fight against the rising antibiotic resistance. Moreover, *P. aeruginosa* is a nefarious opportunistic pathogen that causes various nosocomial and urinary tract infections. *P. aeruginosa* possesses several quantifiable traits such as exopolysaccharides (EPS), biofilm, phenazine, rhamnolipid, pyocyanin and pyoverdin production that directly imparts its pathogenicity. Therefore, any reduction in the quantities of these metabolites has a direct implication on the reduction of its pathogenicity. All these traits are governed by the mechanism of quorum sensing (QS), which in turn is reliant on the signalling protein-ligand interactions. When the growth of *P. aeruginosa* achieves a threshold cell density, the concentration of its signalling QS proteins increases thereby activating a cascade of biochemical reactions leading to the production/manifestation of quantifiable traits. At a high cell density, these bacteria produce signalling molecules, broadly classified as a family of molecules named N-acylated homoserine lactones (AHLs) which are autoinducers (AIs) which is the crux for governing QS (Kalia et al., 2019). In *Pseudomonas*, there are several QS pathways of which, the most obvious are (i) LasR, a protein receptor that identifies an AHL, N-(3-oxododecanoyl)-L-homoserine lactone (OdDHL) that leads to the production of biofilm and EPS; (ii) PhzR, similarly identifies N-hexanoyl-L-homoserine lactone (HHL) and induces phenazine, pyocyanin and pyoverdin production and lastly; (iii) RhlR identifies N-butyryl-L-homoserine lactone (BHL) and activates pathways that synthesizes rhamnolipid. Importantly, it is observed that the concentration of OdDHL, HHL and BHL reaches the threshold at a higher cell density which imparts sudden burst in the yield of biofilm, EPS, phenazines and rhamnolipids which significantly increases its pathogenicity (Lee and Zhang, 2015; Li and Lee, 2019; Shukla et al., 2020). These pathways are interconnected and are represented in Fig. 1.

* Corresponding author.
E-mail addresses: ashukla@gujaratuniversity.ac.in, arpit.shukla@iar.ac.in (A. Shukla), paritoshparmar@gujaratuniversity.ac.in (P. Parmar), patelbaldev56@yahoo.in (B. Patel), dweipayan.goswami@gujaratuniversity.ac.in (D. Goswami), msaraf@gujaratuniversity.ac.in (M. Saraf).

https://doi.org/10.1016/j.micres.2021.126863
Received 18 July 2020; Received in revised form 1 September 2021; Accepted 6 September 2021
Available online 9 September 2021

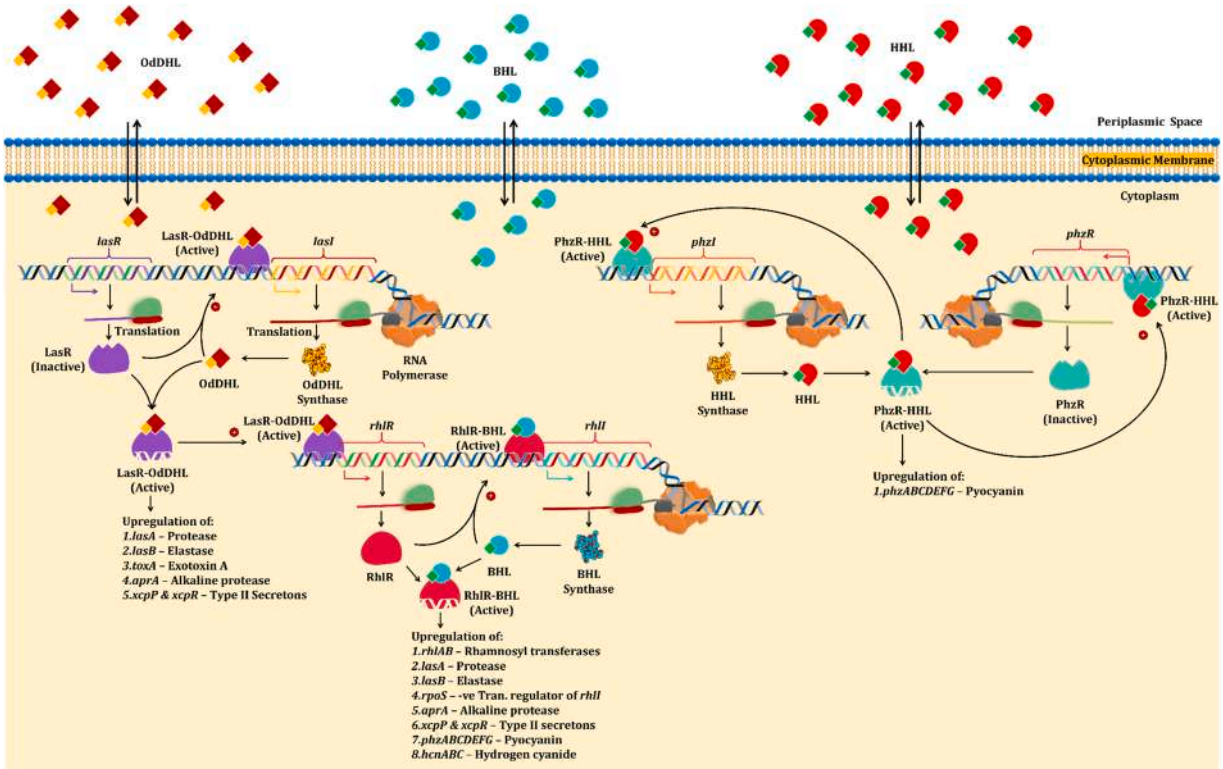

Fig. 1. QS pathways in *P. aeruginosa* (OdDHL: N-(3-oxododecanoyl)-L-homoserine lactone; HHL: N-hexanoyl-L-homoserine lactone; BHL: N-butyryl-L-homoserine lactone).

Antibiotics are compounds that are used to control microbes which may not interfere with QS pathways, but different classes of antibiotics act uniquely by either disrupting the molecular processes of replication, transcription, and translation and even cell disruption. Over the course of time, microbes have evolved by developing various mechanisms to overcome the implications of antibiotics (Ali et al., 2018; Marini et al., 2015). As the microbes develop resistance, higher doses of antibiotics are required to achieve desirable suppression. A time is not so far when a human body may not be able to acquire a dose of antibiotic required to curb a disease caused by such a microbe. The possible approach is to identify newer antibiotics against which the bacteria has not developed resistance, but this approach seems to be far-fetched. There is a need to find an alternative strategy to judiciously use the sensitive antibiotics before they become resistant. Combinational use of two or more antibiotics are employed which is providing overwhelming results for certain microbes while there are reports that such an approach can drive a microbe to evolve resistance against multiple antibiotics in a short span of time. Therefore, there is a need to identify the novel strategy which weakens the virulence of the microbes.

QS-inhibitors (QSI) are molecules which interfere with QS pathways thereby making the community of growing bacteria more vulnerable to the external treatment (Ahmed et al., 2019). To name few QSI that are identified with limited knowledge are gingerol, shogaol and zingerone (phytochemicals of ginger); capsaicin (phytochemical of red chili pepper) and curcumin (phytochemical of turmeric) (Shukla et al., 2020; Kim et al., 2015; Ham et al., 2019; Parmar et al., 2020; Koh et al., 2013). Since these QSI possess the potential to weaken the armoury of the microbial community, their use along with an antibiotic may be employed to achieve better control of microbes using lower concentrations of antibiotic which forms the rationale of present study.

The study is designed to first screen the best QSI which show multifaceted traits of interacting with three different pathways of *P. aeruginosa* governed by AHL-receptors LasR, PhzR and RhlR respectively (Fig. 1). For this purpose, the computational approach was employed which made the use of ligand-receptor docking followed by, validating its result using molecular dynamics, which enables the study of ligand-protein interaction behaviour under simulated environment. Such an approach provides a high degree of surety that the chosen ligand also behaves similarly in *in vitro* environment. To revalidate the computational deductions, *in vitro* studies were performed. The basis of *in vitro* studies was built on grounds to quantify the reduction or suppression of (i) biofilm and EPS production (ii) pyocyanin production and (iii) rhamnolipid production which may be attributed by improper functioning of LasR, PhzR and RhlR respectively, in the presence of identified ligand. Members of *Pseudomonas* spp. have shown to withstand concentrations of antibiotics by an astounding thousand-fold as compared to their non-biofilm producing counterparts (Ali et al., 2018; Marini et al., 2015). Hence, it is imperative to study the molecular basis behind QS, which regulate the formation of biofilm and can be exploited to counter the increasing menace of multi-drug resistance by virulent and pathogenic strains thereby increasing their antibiotic susceptibility. Moreover, in present study, the impact of antibiotic supplementation on *P. aeruginosa* cultivated in presence and in absence of QSI was quantified with an objective to identify the modulation in the antibiotic susceptibility when the microbes' inherent QS pathways are hindered. This study will provide new basis of using an integrated approach of microbial control aided by QSI's with antibiotic.

2. Materials and methods

2.1. Homology modelling and comparison of LasR, PhzR and RhlR

From the three proteins used under present study, the crystal structure of only LasR is available on protein databank (PDB) while the other two proteins are not yet crystallized. The crystal structure of LasR used for the present study was retrieved from PDB (ID: 2UV0) while PhzR and RhlR structures were modelled using the protein sequence available from UniProt with an ID: Q51786 and P5429, respectively. Both these

proteins were modelled using SWISS-MODEL where, for PhzR and RhlR, the template used were 4Y15.2.A and 4Y15.2.B respectively, which are two different chains of same protein 4Y15 of PDB. The quality analysis of the predicted model was performed using QMEAN and QMEANDisCo scores of modelled proteins was performed using SWISS-MODEL server (Benkert et al., 2011). The Ramachandran plot analysis was performed using MolProbity v4.4 to check the psi (ψ) and phi (ϕ) angles of the modelled PhzR and RhlR to check the overall torsion of the residues. Further, ERRAT analysis was performed to reliably identify the regions of error in predicted protein crystal structure by examining the statistics of pairwise atomic interactions (Colovos and Yeates, 1993). Owing to the similar function of all these three proteins, their structures possess identical traits which can be easily observed on superimposing all three proteins. The LasR x-ray crystal structure resolution was of 1.80 Å (PDB ID: 2UV0) and is a homotetramer comprised of chains E, F, G and H of which only chain E was used for further studies. Therefore, only a single chain of PhzR and RhlR were modelled. The hydrophobic cavity consisting of active site of all three proteins were identified using Needleman-Wunsch alignment algorithm with BLOSUM-62 matrix and iterate pruning long atom pairs until 2.0 Å was chosen as a parameter in MatchMaker tool of UCSF Chimera v1.13 (Pettersen et al., 2004). The superimposed proteins were saved as a single PDB file and were visualized in BIOVIA Discovery Studio (DS) 2019 R1 and the superimposition of the active sites was studied. Moreover, all three proteins share the same structural features might have different origins that can be studied by comparing and observing their proteins sequences, for which CLUSTAL Omega algorithm of multiple sequence alignment was employed.

2.2. Screening of QSI's for LasR, PhzR and RhlR using docking

The protein **LasR** was retrieved from Protein databank (PDB), ID 2UV0 which existed as a homodimer. Prior to docking studies, all the co-crystallized residues were removed in UCSF Chimera and only one chain was used for further studies. The protein structure was then prepared by assigning the hydrogen atoms, charges and energy minimization using DockPrep tool (Krivov et al., 2009). The charges were assigned as per the AM1-BCC method which quickly and efficiently generates high-quality atomic charges for protein and the charges were computed using ANTECHAMBER algorithm (Wang et al., 2001). The energy minimization was performed using 500 steepest descent steps with 0.02 Å step size and an update interval of 10. All the steps mentioned were performed in Chimera. All the ligands used for the *in-silico* interaction assays were reported analogs of AHL which were retrieved from PubChem. For docking, the ligands were optimized by addition of hydrogen and energy minimization using Gasteiger algorithm (Gasteiger and Jochum, 1979) in structure editing wizard of Chimera, which works on the chemoinformatic principle of electronegativity equilibration and the files were saved in mol2 format. Receptor-ligand Docking analysis was performed using AutoDock Vina and the program was executed as an add-on in Chimera (Trott and Olson, 2010). For docking, following parameters were set as: (i) number of binding modes- 10; (ii) exhaustiveness of search- 8 and (iii) maximum energy difference- 3 kcal/mol. Out of all the possible poses suggested by AutoDock Vina, the pose showing maximum hydrogen bonds and minimum binding free energy change (kcal/mol) as represented in the ViewDock window were chosen. They were further analysed in Biovia Discovery Studio (DS) visualizer for hydrogen bond formation by the functional groups of ligands with amino acids (Rao et al., 2020).

2.3. Molecular Dynamics (MD) for simulation studies

The simulations were performed using GROMACS 2019 (Pronk et al., 2013; Van Der Spoel et al., 2005; Bekker et al., 1993). The topology of the ligand was generated using SwissParam, which provides topology and parameters for small organic molecules compatible with the CHARMM all atoms force field, for use with CHARMM and GROMACS (Zoete et al., 2011). Whereas the topology of the protein was created using GROMACS utilities using CHARMM27 all-atom force field (CHARM22 plus CMAP for proteins) with the water model set to TIP 3-point. The structure (Ligand-protein complex) were defined with unit cell box under periodic boundary conditions using 1.0 nm distance from the protein to the box faces with triclinic shape and was filled with water (Berendsen et al., 1981). This was then followed by neutralization by Cl^- or Na^+ counter ions. Steepest descent energy minimization was performed, and the systems were equilibrated under NVT (constant number of particles, volume, and temperature) conditions for 100 ns at 300 K. Once the NVT run was completed the system was proceeded with NPT (constant number of particles, pressure, and temperature) Simulation and MD run was performed for 100 ns. All the covalent bonds were constrained using the LINCS (Linear Constraint Solver) algorithm (Hess et al., 1997). The electrostatic interactions were treated using the Particle Mesh Ewald (PME) method. The cut-off radii for Coulomb and van der Waals interactions were set to 10.0 and 14.0 Å, respectively. On completion of NVT and NPT Simulation, the potential of each trajectory produced were analysed. Trajectories were analysed for root-mean-square deviation (RMSD), root-mean-square fluctuation (RMSF), radius of gyration (Rg) and the number of H-bonds formed between the ligand and proteins using 'gmx rms','gmx rmsf', 'gmx gyrate' and 'gmx hbond' of GROMACS utilities (Pronk et al., 2013; Bekker et al., 1993). Ligand–protein stability was determined by the Dynamics of hydrogen bonds between ligand and protein with respect to time. XMgrace tool was used to prepare the graphs (Turner, P.J.C.f.C. et al., 2005).

2.4. ADMET analysis

The pkCSM - pharmacokinetics server (Pires et al., 2015) was used to predict the ADMET (drug absorption, distribution, metabolism, excretion and toxicity) properties of the best ligand. It predicted both physiochemical and pharmacological properties. SMILES (Simplified Molecule Input Line Entry Specification) of the compounds were retrieved from PubChem and uploaded to pkCSM - pharmacokinetics server. It computed *in-vivo* Absorption parameters like, Water solubility in buffer system (SK atomic types, mg/L), *in-vivo* Caco2 cell permeability (Human colorectal carcinoma), Human intestinal absorption (HIA, %), *in-vivo* P-glycoprotein inhibition and *in-vivo* skin permeability (logKp, cm/hour). Metabolic parameters were determined using *in-vivo* Cytochrome P450 2C19 inhibition, *in-vivo* Cytochrome P450 2C9 inhibition, *in-vivo* Cytochrome P450 2D6 inhibition, *in-vivo* Cytochrome P450 2D6 substrate, *in-vivo* Cytochrome P450 3A4 inhibition and *in-vivo* Cytochrome P450 3A4 substrate, Distribution property included tests like, Blood-Brain Barrier (BBB) penetration, Lipinskis Rule (Rule of Five), Central Nervous System (CNS) permeability. While, toxicity properties covered a range of important endpoints including, Acute algae toxicity, Ames test, 2 years carcinogenicity bioassay in mouse, 2 years carcinogenicity bioassay in rat, *in-vivo* Ames test result in TA100 strain (Metabolic activation by rat liver homogenate) were computed to access the toxicity of compounds under study. Excretion again is a very important parameter and as many drugs often withdrawn at clinical trial stages due to their poorer renal clearance. In this study we included Total Renal clearance and Renal OCT2 Substrate to identify Excretion efficacy of the proposed metabolite (Rao et al., 2020).

2.5. In vitro assessment on EPS, biofilm, pyocyanin, rhamnolipid and antibiotic susceptibility on P. aeruginosa

To test our hypothesis, previously isolated *P. aeruginosa* AM26 (GenBank accession no.: MN871520) showing high degree of genetic similarity with *P. aeruginosa* PAO1 was chosen for the *in vitro* studies. Gingerol (Sigma-Aldrich) was procured and was used to perform various assays. Biofilm assay was performed in presence and absence of gingerol

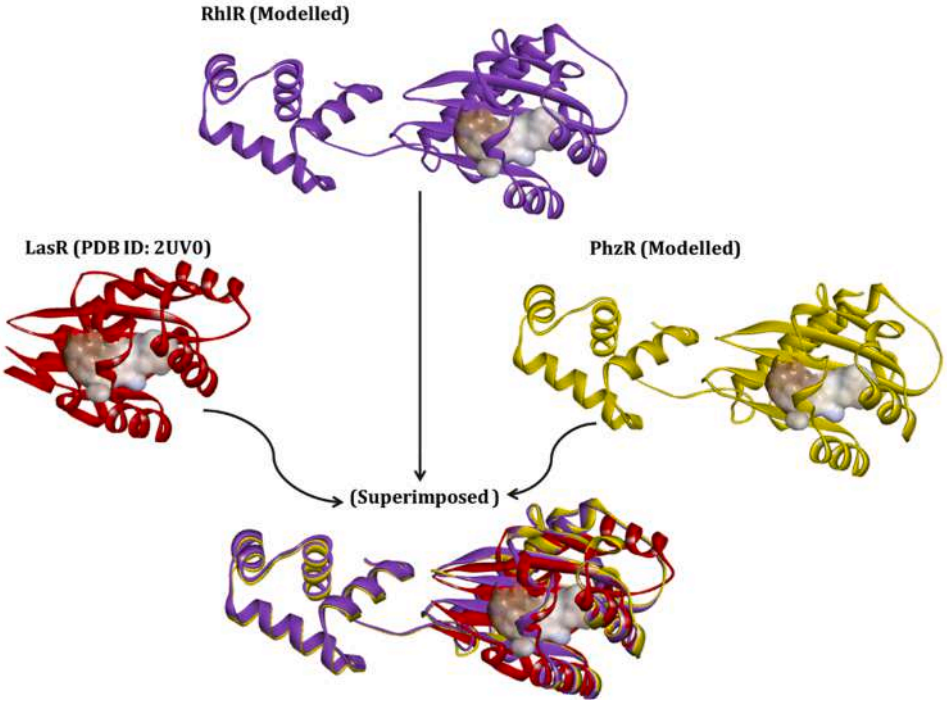

Fig. 2. Structure comparison of various AHL receptors of *Pseudomonas aeruginosa*. Protein LasR is co-crystallized (PDB ID: 2UV0) while 3D structures of RhlR and PhzR are developed using homology modelling. Image representing identical AHL binding cleft in all three proteins.

to verify the results of molecular docking studies. The biofilm assay was performed in microtiter plate as per the method described by O'Toole (O'Toole, 2011) without any modifications. For tests with gingerol, same conditions were employed with additionally varying the concentrations of gingerol in the range of 10–50 μg/mL in different sets while, the control run was devoid of gingerol supplementation. For EPS production, the culture was grown in the nutrient broth supplemented with sucrose (3 g% w/v). Culture flasks were inoculated with 5 %(v/v) inoculum of actively growing culture and could grow for 144 h at 30 ± 2 °C by providing constant agitation of ~150 rpm on an orbital shaker. The production broth was centrifuged at 10,000 rpm for 20′ at 4 °C and the pellet was dissolved in 3 times the volume of chilled acetone for precipitation of EPS and to enhance the precipitation, this mixture was left overnight at 4 °C. The precipitated EPS was recovered using centrifugation and could dry for removal of moisture to a constant weight. The production of EPS was represented in terms of g % (w/v) (Shukla et al., 2019). Crude pyocyanin was initially extracted from 72 h old culture grown in nutrient broth. The culture supernatant was recovered by centrifugation at 5000 *g*. For assaying pyocyanin activity, 5 mL supernatant of the trichloroacetic acid containing samples with 3 mL of chloroform. To this, 1 mL of 0.2 N HCl was added to recover pyocyanin. This was then estimated by measuring OD at 520 nm spectrophotometrically and the results are represented as pyocyanin activity by normalizing it using culture cell density at 600 nm. For assaying rhamnolipid activity, the 72-h old same culture was used. Crude rhamnolipid was initially extracted twice by mixing 500 mL cell supernatant of overnight culture with 1 mL of diethyl ether which was then evaporated to dryness. The dry extract was eluted in 500 mL deionized water, and 1 mL of the elution was mixed with 9 mL orcinol solution (solution prepared by adding 0.19 g orcinol in 100 mL of 10 N H_2SO_4). The mixture was boiled for 30 min for reaction to occur which gives orange-red colour, and then cooled at room temperature. The colour developed was recorded spectrophotometrically at 421 nm. The results are represented as rhamnolipid activity by normalizing it using culture cell density at 600 nm. To study the impact of gingerol on antibiotic susceptibility, two sets of experiments were performed by supplementing different concentrations of antibiotic (ciprofloxacin), ranging from 0.5 to 2.5 μg/mL in the culture broth of *P. aeruginosa*. While in the other set, an additional 30 μg/mL of gingerol was supplemented in all the culture flasks with varying concentrations of antibiotic. The growth achieved by the culture after 24 h was recorded spectrophotometrically at 600 nm. The maximum growth achieved in two different sets (with and without gingerol), with same antibiotic concentration were compared to deduce the impact of gingerol on the effectiveness of the antibiotic.

3. Results

3.1. Homology modelling and comparison of LasR, PhzR and RhlR

The crystallized 3D model of LasR was retrieved with PDB (ID: 2UV0) while PhzR and RhlR were modelled using SWISS-MODEL which was based on chain B and chain A of PDB ID 4Y15.2 as template. The model quality assessment of PhzR showed its QMEAN value to be -3.6 and Global Model Quality Estimation (GMQE) value was 0.75. The Ramachandran plot analysis was done using MolProbity v4.4, suggested 94.89 % of residues falling in the favoured region whereas, the 1.01 % rotamer outliers were Val52 and Asn221 while 2.13 % Ramachandran outliers were Pro95, Pro125, Ser117 and Ala94. Out of 3870 bonds found in the model, none showed discordant bond in MolProbity analysis. The overall MolProbity score was found to be 1.73. Similarly, the quality assessment of RhlR was as follows: (i) QMEAN score -2.04, (ii) GMQE value 0.77, (iii) Ramachandran analysis suggested 96.58 % of residues falling in the favoured region whereas, the 1.46 % rotamer outliers were Leu130, Pro20 and Asn218 while 0.85 % Ramachandran outliers were Pro123 and Ile143, (iv) out of 3894 bonds found in the model, one amino acid (Gly6) showed discordant bond in MolProbity analysis. The overall MolProbity score was found to be 1.61.

The structure analysis suggested that, LasR lacked the HTH domain while PhzR and RhlR possessed it. The sequence similarity of these three proteins despite being devoid of similarity possessed very high degree of structural similarity. This can be visualized by superimposing all these

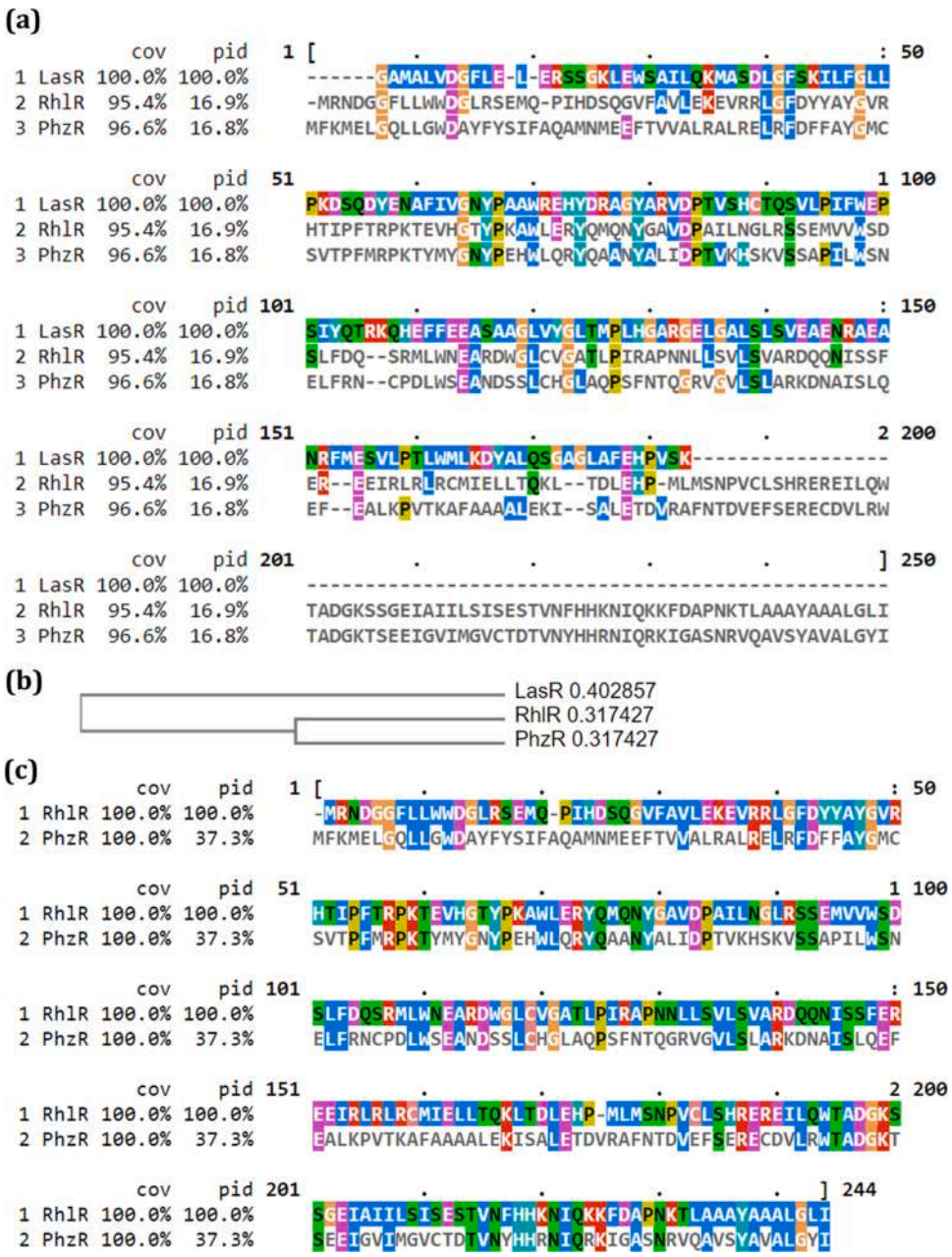

Fig. 3. (a) Multiple sequence alignment of LasR, RhlR and PhzR (b) Phylogenetic relationship between LasR, RhlR and PhzR (c) Multiple sequence alignment of structurally identical and phylogenetically related proteins, RhlR and PhzR.

three proteins represented in Fig. 2. The structural analysis further suggested that, the active sites of all three proteins were identical consisting of a five-stranded antiparallel β-sheet packed against three α-helices on each side. The cavity was found to be formed by a cluster of hydrophobic and aromatic residues. Superimposition of all proteins show the identical ligand-binding cleft, therefore, may have similar ligand binding properties. Although, these proteins having structural identity show poor sequence similarity (Fig. 3). PhzR and RhlR showed the sequence similarity of ~40 % and LasR had only ~19 % similarity with PhzR and RhlR. This suggests that all three proteins might have different lineage, but they share striking identical structural and functional relationship.

3.2. *Screening of QSI's for PhzR and RhlR using docking*

Using the *in-silico* approach, the interactions of LasR, PhzR and RhlR with native ligands and naturally occurring proposed QSIs (capsaicin, gingerol, shogaol, zingerone, curcumin and quercetin) were studied to find the best fit QSI that could cumulatively interact with these AHL-receptors. The cognate ligand, OdDHL, makes five H-bonds with Tyr56, Trp60, Arg61, Asp73 and Ser129 of LasR while making hydrophobic interactions with Leu40 and Ala50 in the form of alkyl and pi-alkyl bonds. The spontaneity of this binding is represented by free energy change of -8.9 kcal/mol. (Fig. 4a). Of all the ligands tested for QSI ability, gingerol has shown to make the most spontaneous interactions with LasR with the binding free energy of -8.6 kcal/mol by making H-bonds with Tyr56, Arg61, Thr75, and Thr115 moreover, it is shown to make many more hydrophobic interactions by interacting with Leu36, Ala127, Val76, and Cys79 (Table 1). The pattern of interaction by gingerol with LasR is different than that of OdDHL. This can make the protein change its conformation and may render it ineffective. Similarly, when the docking was performed with all the proposed QSIs, gingerol

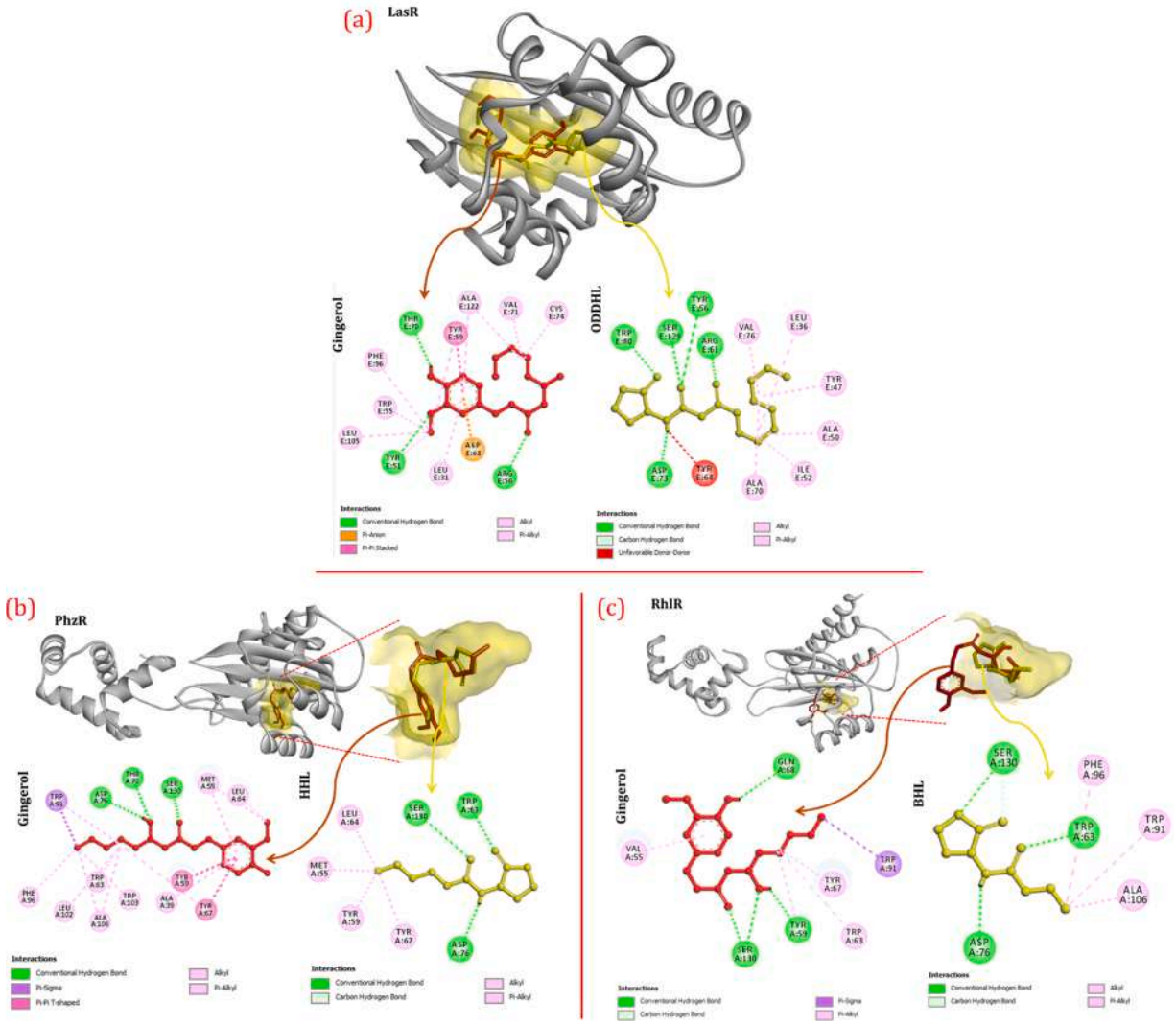

Fig. 4. Computationally predicted interactions of cognate ligand and gingerol with (a) LasR, (b) PhzR and (c) RhlR where, 3D orientations of ligand in the binding cleft of the proteins are depicted along with their interactions with amino acids represented in 2D cartoons.

was found to be most efficient in binding with RhlR and PhzR based on binding free energy change along with formation of H-bonds and hydrophobic interactions. For PhzR, its native ligand HHL showed to make three H-bonds with Trp63, Asp76 and Ser130 along with making few hydrophobic interactions with Met55, Tyr59, Leu63 and Tyr67 (Fig. 4b). For RhlR, its cognate ligand BHL was also found to be making three H-bonds with Trp63, Asp76 and Ser130 while additionally making three hydrophobic interactions with Trp91, Phe96 and Ala106 (Fig. 4c). For both these proteins, their native ligand could make maximum three H-bonds and three to four hydrophobic interactions each. Surprisingly, gingerol could interact even more strongly with both these proteins by making three to four H-bonds with many more hydrophobic interactions. Gingerol formed H-bonds with Asp76, Thr78 and Ser130 along with making thirteen different hydrophobic interactions with the amino acids of PhzR (Table 1). In case of Rhl, similar phenomenon was observed where H-bonds were formed with Tyr59, Gln68 and Ser130 (which could participate to make two H-bonds) while making five hydrophobic interactions (Table 1). Thus, of all the reported QSIs, gingerol was inferred to be the best and could interact with AHL receptors at par or even better than their cognate counterparts. Based on the structural differences, gingerol can serve as an antagonist but not an agonist as it may modify the 3D conformation of the active protein to make it ineffective.

Structure comparison of gingerol with different AHLs suggests that, gingerol is ~30 % larger in size along with ~40 % greater surface area when compared to the largest AHL (HHL) (Table 1). Moreover, AHL and gingerol share certain similar structural features. Gingerol possess a hydroxyl group at the 5-position, a carbonyl group at the 3-position, and a 4′-hydroxy-3′-methoxy phenyl group at 1-position of its decane backbone structure along with possessing a long alkyl chain showing analogy to AHLs. However, the terminal aromatic nature of gingerol distinguishes it from AHLs.

3.3. Molecular dynamics (MD)

To affirm the docking studies, simulations in the cellular environment was performed computationally using molecular dynamics to provide an insight regarding the stability of ligand receptor interactions with respect to time. Three sets of protein-ligand interaction were studied with each set comprising of two simulations, one with its cognate ligand and another with gingerol (as gingerol showed most efficient binding in docking studies). In total of six simulations were performed using GROMACS. Root Mean Square Deviation (RMSD), Root Mean Square Fluctuation (RMSF) and H-bonds were computed for each simulation run of 100 ns to gauge the stability of protein-ligand interaction. RMSD is used to analyse the equilibration of MD trajectories.

Table 1
Molecular Properties of ligands of AHL-receptors used under study (merge with docking table).

Ligand name	H-bond interactions	Hydrophobic interactions	Energy (kcal/mol)
LasR			
OdDHL	Tyr56, Trp60, Arg61, Asp73, Ser129	Leu40, Ala50	−8.9
Capsaicin	Asp68, Ser124, Leu105	Trp83, Phe96, Ala100, Leu35, Ala45,	−9.2
Gingerol	Tyr56, Arg61, Thr75, Thr115	Leu36, Ala127, Val76, Cys79	−8.6
Shogaol	Tyr41, Thr109, Ser123	Leu30, Ala44, Val70, Tyr58, Trp82	−8.2
Zingerone	Tyr50, Arg55, Thr69, Thr109	Tyr58, Leu30	−7.2
Curcumin	Arg56, Leu105, Leu120	Trp83, Phe96, Ala100, Leu35, Ala45, Gly121, Gly33, Val71, Asp68	−10.0
Quercetin	Try42, Tyr51, Gly121	Val71, Ala122, Tyr59	−10.6
PhzR			
HHL	Asp76, Thr63, Ser130	Tyr67, Tyr59, Met55, Leu64	−7.0
Capsaicin	Trp63	Ala39, Met55, Tyr59, Tyr67, Ala73, Val79, Asp76	−6.7
Gingerol	Asp76, Thr78, Ser130	Trp91, Tyr59, Tyr67, Met55, Ala39, Phe96, Trp103	−6.7
Curcumin	Trp63	Met55, Asp76, Tyr67	−7.7
Shogaol	Trp63 (2)	Met55, Asp76, Tyr67, Val76, Cys43	−6.8
Zingerone	–		−6.5
Quercetin	Tyr59, Tyr67, Ser130	Met55, Asp76, Val79, Gly41	−6.2
RhlR			
BHL	Trp63, Asp76, Ser130		−6.5
Capsaicin	Ala39, Ser130	Tyr67, Ile79, Val55, Tyr59, Val128, Asp76	−7.5
Gingerol	Tyr59, Gln68, Ser130	Trp91, Ala78, Phe96, Val55	−7.5
Shogaol	Gln68, Ser130	Trp91, Ala78, Val55, Phe96, Leu102	−7.6
Zingerone	Trp63, Val128, Ser130	Ala39, Val55	−6.7
Curcumin	Gly41	Val55, Try67, Trp63, Tyr59, Ala39	−8.6
Quercetin	Gln68, Ser130	Val55, Tyr67, Asp76, Ala78	−8.7

Molecular properties of Gingerol (first ranked ligand), OdDHL, BHL and HHL

Descriptor	Gingerol	OdDHL	BHL	HHL
Molecular Weight	294.391	213.233	171.196	217.265
LogP	3.2338	0.1774	0.2182	0.5185
#Rotatable Bonds	10	5	3	8
#Acceptors	4	4	3	3
#Donors	2	1	1	3
Surface Area	126.309	88.166	71.274	89.485

Here, the stability of the protein backbone while interacting with ligand is represented using RMSD and are plotted as a function of time (Fig. 5a–c). The plots of RMSDs are constructed by superimposing the curves of gingerol (red) on native ligand (black). RMSD values below 1 are ideal suggesting no hindrance in the stability of the complex. All the RMSD graphs shows the value below 0.3 reflecting the stability of all three proteins in presence of gingerol as well as their cognate ligands. In a general term, the RMSD values for all the three proteins interacting with gingerol there is slightly a higher value due to its larger size and the surface area as compared to its native ligand. RMSF indicates the flexibility differences in the residues of the protein backbone. Here, the purpose of assessing RMSF is to determine the flexibility in the residues of protein backbone in presence of native ligand *vs* gingerol. Higher the RMSF, greater is the entropy and less is the stability. This deduces the stabilizing effect of ligand on protein. The RMSF values of all the proteins in presence of native ligand and gingerol is depicted in Fig. 5d–f by superimposing the curves of gingerol (red) on native ligand (black). The identical curves superimposing depicts the identical RMSF values of proteins interacting with gingerol and their native ligands. This shows that gingerol imparts no instability in the residues of these proteins during its interaction.

The purpose of performing a molecular dynamics is to reassure that the number of H-bonds shown to be formed during docking study should remain consistent during simulation. Any instability caused by improper pose of the ligand may not be reflected in the docking but could be easily reflected during simulation. In such a case, the number of H-bonds formed during simulation will reduce and will be lesser than that proposed during docking. The H-bond formed by each ligand with protein is depicted in Fig. 5g–l and it reassures the same number of H-bonds are formed in simulation as were predicted by docking. All the AHLs were consistently able to make an average of three H-bonds at any given time during simulation owing to the fact the life of one H-bond being $\sim 10^{-9}$ ps and the similar phenomenon was also observed for gingerol during its interaction with all three proteins (Nelson et al., 2008).

3.4. ADMET analysis

Gingerol has shown promise to serve as a major participant in the integrated approach for microbial control, its drug properties were assessed using ADMET (drug absorption, distribution, metabolism, excretion, and toxicity) properties. All the major properties are represented in Table 2, it is observed that it does not show any hepatotoxicity, has high intestinal absorption, high value of distribution in body, does not possess skin sensitivity and it does not follow the Lipinski's rule of five by which it is not predicted to pass the blood-brain barrier as its logBB < 0.3. Maximum Tolerated Dose (MRTF) is found to be greater than 0.477 log(mg/kg/day) therefore, the tolerance is found to be high for the body proving it to be less toxic. hERG I and II are potassium channels that, when hindered, causes QT syndrome (Q and T peaks of electrocardiograms are distorted), here, gingerol is not shown to interact with hERG receptors thus it is safe for people with heart conditions. Hence, from ADMET properties, gingerol has desirable drug-like properties being safe for consumption.

3.5. In vitro assessment

Gingerol, along being considered as QSI is also reported to inhibit the growth of bacteria. To assess the QSI properties of gingerol, it is essential to identify the concentration range which bacteria can withstand without getting inhibited which can be termed as the working range (WR). All the QSIs experiments, that is to identify biofilm, EPS, pyocyanin and rhamnolipid production and antibiotic susceptibility assays

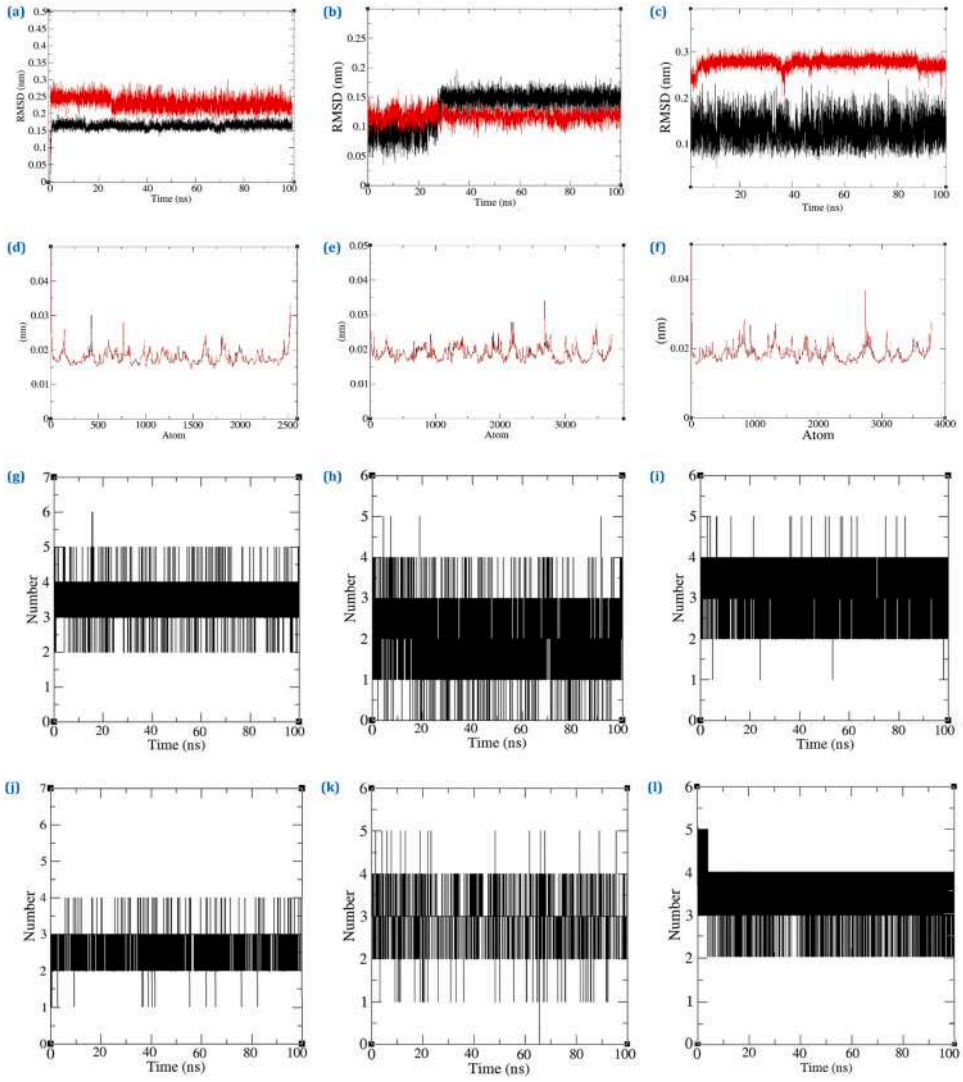

Fig. 5. Results of molecular dynamics where, RMSDs (a-c) of backbone during interaction with cognate ligand-black and gingerol-red (a) LasR (b) PhzR and (c) RhlR. RMSF values (d-f) of protein (d) LasR (e) PhzR and (f) RhlR backbones while interacting with cognate ligand-black and gingerol-red. H-bonds (g-l) formed by ligand with the proteins is depicted (g) OdDHL with LasR (h) gingerol with LasR (i) HHL with PhzR (j) gingerol with PhzR (k) BHL with RhlR and (l) gingerol with RhlR.

were performed within this gingerol WR. To identify the WR, growth assessment of *P. aeruginosa* AM26 was performed by supplementing 10–50 μg/mL gingerol in the culture broth. It was observed that there was no significant decrease in growth up to 30 μg/mL of gingerol in the culture medium and even at 50 μg/mL, significant growth of culture was observed (Fig. 6a). The growth curve of the bacterium depciting correlation between OD and CFU/mL cell count on nutrient medium is provided in supplementary file (S1). The biofilm assay was performed to deduce the suppression of LasR by gingerol and it was observed that, at 30 μg/mL the biofilm production was reduced by 30 % (Fig. 6b) however, at this concentration, no significant reduction in the growth was observed (Fig. 6a). Another experiment of EPS production was performed to assess the operation of LasR in presence of gingerol where it was observed that, at 30 μg/mL there was ~40 % decrease in the EPS yield (Fig. 6c). As LasR is central regulatory pathway which also controls PhzR and RhlR, the cumulative suppression of all these proteins especially PhzR was assessed by pyocyanin production assay where it was observed that, the culture's ability to produce pyocyanin was reduced by ~40 % in presence of 30 μg/mL gingerol (Fig. 6d). The production of rhamnolipid is coregulated by RhlR and LasR but more specifically by RhlR and therefore, impact of gingerol on the culture's ability to produce rhamnolipid was assessed. It was observed that, there was reduction by 20 % in the rhamnolipid production at 30 μg/mL of gingerol. From all the assays to study the impact of gingerol on inhibiting the QS pathways, its concentration of 30 μg/mL (Fig. 6e) was considered as the gold standard as at this concentration the growth was not hindered but the QS pathways were suppressed. Therefore, effect of gingerol on antibiotic susceptibility was performed using 30 μg/mL of gingerol in the culture medium with different concentrations of ciprofloxacin antibiotic. It was observed that, the potency of the antibiotic was enhanced in presence of gingerol where at least 20 % of the growth was suppressed in the minimal concentration of ciprofloxacin supplemented (0.5 μg/mL). Moreover, it was observed that the antibiotic susceptibility was almost doubled at 1.0 μg/mL of ciprofloxacin (Fig. 6f). Thus, from all the *in vitro* assays it was deduced that: (i) at 30 μg/mL gingerol was able to suppress multiple QS driven production of biomolecules without any significant suppression in growth and, (ii) the increased susceptibility of antibiotic on *P. aeruginosa* AM26 in presence of gingerol suggesting the inherent weakening of the bacterium when their QS pathways are hindered.

4. Discussion

Pseudomonas aeruginosa is one of the most widely studied organisms,

Table 2
ADMET properties of Gingerol.

Property	Model Name	Predicted Value (Gingerol)	Unit
Absorption	Water solubility	**−3.164**	Numeric (log mol/L)
Absorption	Caco2 permeability	**0.94**	Numeric (log Papp in 10^{-6} cm/s)
Absorption	Intestinal absorption (human)	**92.416**	Numeric (% Absorbed)
Absorption	Skin Permeability	**−2.817**	Numeric (log Kp)
Absorption	P-glycoprotein substrate	**Yes**	Categorical (Yes/No)
Absorption	P-glycoprotein I inhibitor	**No**	Categorical (Yes/No)
Absorption	P-glycoprotein II inhibitor	**No**	Categorical (Yes/No)
Distribution	VDss (human)	**0.524**	Numeric (log L/kg)
Distribution	Fraction unbound (human)	**0.258**	Numeric (Fu)
Distribution	BBB permeability	**−0.727**	Numeric (log BB)
Distribution	CNS permeability	**−2.788**	Numeric (log PS)
Metabolism	CYP2D6 substrate	**No**	Categorical (Yes/No)
Metabolism	CYP3A4 substrate	**No**	Categorical (Yes/No)
Metabolism	CYP1A2 inhibitor	**Yes**	Categorical (Yes/No)
Metabolism	CYP2C19 inhibitor	**Yes**	Categorical (Yes/No)
Metabolism	CYP2C9 inhibitor	**Yes**	Categorical (Yes/No)
Metabolism	CYP2D6 inhibitor	**No**	Categorical (Yes/No)
Metabolism	CYP3A4 inhibitor	**No**	Categorical (Yes/No)
Excretion	Total Clearance	**1.339**	Numeric (log ml/min/kg)
Excretion	Renal OCT2 substrate	**No**	Categorical (Yes/No)
Toxicity	AMES toxicity	**No**	Categorical (Yes/No)
Toxicity	Max. tolerated dose (human)	**0.635**	Numeric (log mg/kg/day)
Toxicity	hERG I inhibitor	**No**	Categorical (Yes/No)
Toxicity	hERG II inhibitor	**No**	Categorical (Yes/No)
Toxicity	Oral Rat Acute Toxicity (LD50)	**1.958**	Numeric (mol/kg)
Toxicity	Oral Rat Chronic Toxicity (LOAEL)	**1.631**	Numeric (log mg/kg_bw/day)
Toxicity	Hepatotoxicity	**No**	Categorical (Yes/No)
Toxicity	Skin Sensitisation	**No**	Categorical (Yes/No)
Toxicity	*T. pyriformis* toxicity	**1.487**	Numeric (log ug/L)
Toxicity	Minnow toxicity	**0.966**	Numeric (log mM)

finds a plethora of applications in PGPR, bioremediation and molecular investigative studies *etc* (Goswami et al., 2015; Goswami et al., 2016). However, being nefarious by causing infections to immune-compromised patients and then being untreatable cause lot of challenges in medical community to curb its infection while flourishing in infection, the greater threat posed by this microbe is its acquired resistance to several antibiotics. Moreover, the rate at which the strains of *Pseudomonas* acquiring resistance to antibiotics is skyrocketing. The need of the hour is therefore, to turn towards targeting different pathways of this microbe to suppress its growth that are currently not being used by conventional antibiotics. The most promising hypothesis is to target its QS pathway.

QS is a phenomenon widely studied in bacteria, where in Gram-negative bacteria this phenomenon is studied in detail. The major group of QS involved autoinducers (AHLs) that serves as a signal which will bind to their receptors. The receptors of Gram-negative QS possess high degree of structural identity but they are originated from different lineages therefore, they share very low levels of sequence similarity (Nasser and Reverchon, 2007). In the present study, we have observed that LasR, PhzR and RhlR possess identical AHL-binding cleft but show very low sequence similarity and these proteins share similar structure, function relationship. Inhibiting the QS pathways has been seen as a new avenue to develop anti-microbial agents as antibiotic resistance is posing a threat to the scientific community and where in identifying new antibiotic is becoming increasingly difficult (Ahmed et al., 2019). Blocking of QS pathways has been proposed to weaken the armoury of microbes thereby making them more vulnerable (Rasmussen et al., 2005). The molecules involved in the strategies to block QS are called Quorum Sensing Inhibitors (QSI) (Koh et al., 2013). Molecular docking and dynamic simulation are one of the most robust approach to study the interaction of protein with small molecules computationally with high accuracy (Shukla et al., 2020; Parmar et al., 2020; Rao et al., 2020).

LasR is the central regulator which controls the production of OdDHL, BHL and RhlR. LasR also activate *lasA, lasB*, *lecA and lecB* genes which are involved in the production of exoprotease, elastase and lectin which are respectively due to the action of LasA, LasB and LecAB. Moreover, RhlR activation further aides the activity of *las* and *lec* gene clusters. Activation of RhlR induces expression of *rhlABC* cluster that produces rhamnolipid. Further, RhlR also induces PhzR production, which on activation by HHL, causes the expression of *phzABCDEFGH* cluster which leads to the production of phenazine and pyocyanin. The ultimate products of LasR, RhlR and PhzR that are EPS, biofilm, rhamnolipid, phenazine and pyocyanin are responsible for imparting virulence (Lee and Zhang, 2015; Nazzaro et al., 2013). Therefore, it is important to break the intricacies of quorum sensing signalling cascade to curb the virulence (Kim et al., 2015).

For the present study, we have made the use of naturally derived QSI which are previously reported by their mode of actions are still being investigated. Owing to this, we have used capsaicin, gingerol, shogaol, zingerone, curcumin and quercetin (Shukla et al., 2020; Kim et al., 2015; Parmar et al., 2020; Rasmussen et al., 2005; Szabó et al., 2010). Moreover, despite their cumulative impact on multiple QS pathways are still to be investigated. As an approach, first we have screened the best QSI molecule based on docking and then for validating the results obtained, molecular dynamics simulations were performed to assess their impact on multiple QS pathways of *P. aeruginosa* driven by LasR, PhzR and RhlR. Moreover, it is observed that suppression in QS decreases the virulence in *P. aeruginosa* but the mechanism is still not understood (Shukla et al., 2020).

Of all the QS pathways to be found in Gram-negative bacteria, the signalling architecture driven by AHL signals, the LasR-LasI system of QS of *P. aeruginosa* is most widely studied and is regarded as the model AHL-induced QS pathway (Lee and Zhang, 2015). Broadly, all these protein receptors of AHL share structural similarity with LuxR protein of *Vibrio fischeri* and hence, they are categorized as LuxR-family of proteins which are vividly portrayed by Nasser and Reverchon (2007) where they have suggested that despite being structurally identical, these proteins may have completely different genetic origin making their protein sequence dissimilar. Under present study, RhlR and PhzR were modelled, and their quality were examined using QMEAN4, GMQE and Ramachandran plot analysis using MolProbity. The results obtained showed the quality of the model built was at par with the parameters for homology modelling published so far (Ali et al., 2018).

The most rigorous efforts to understand the QSI potentials were performed by Kim, Lee (Kim et al., 2015) have also proposed gingerol to possess the ability to down-regulate PhzR and RhlR however, no experiments were performed because their crystalline structures were not available. To fill this loophole, we have furthered their hypothesis by modelling PhzR and RhlR and then performing their docking studies. Down-regulation of the genes that get activated by these receptors were also shown by them using RT-PCR. However, their experiments lacked computational studies which we have performed incorporating

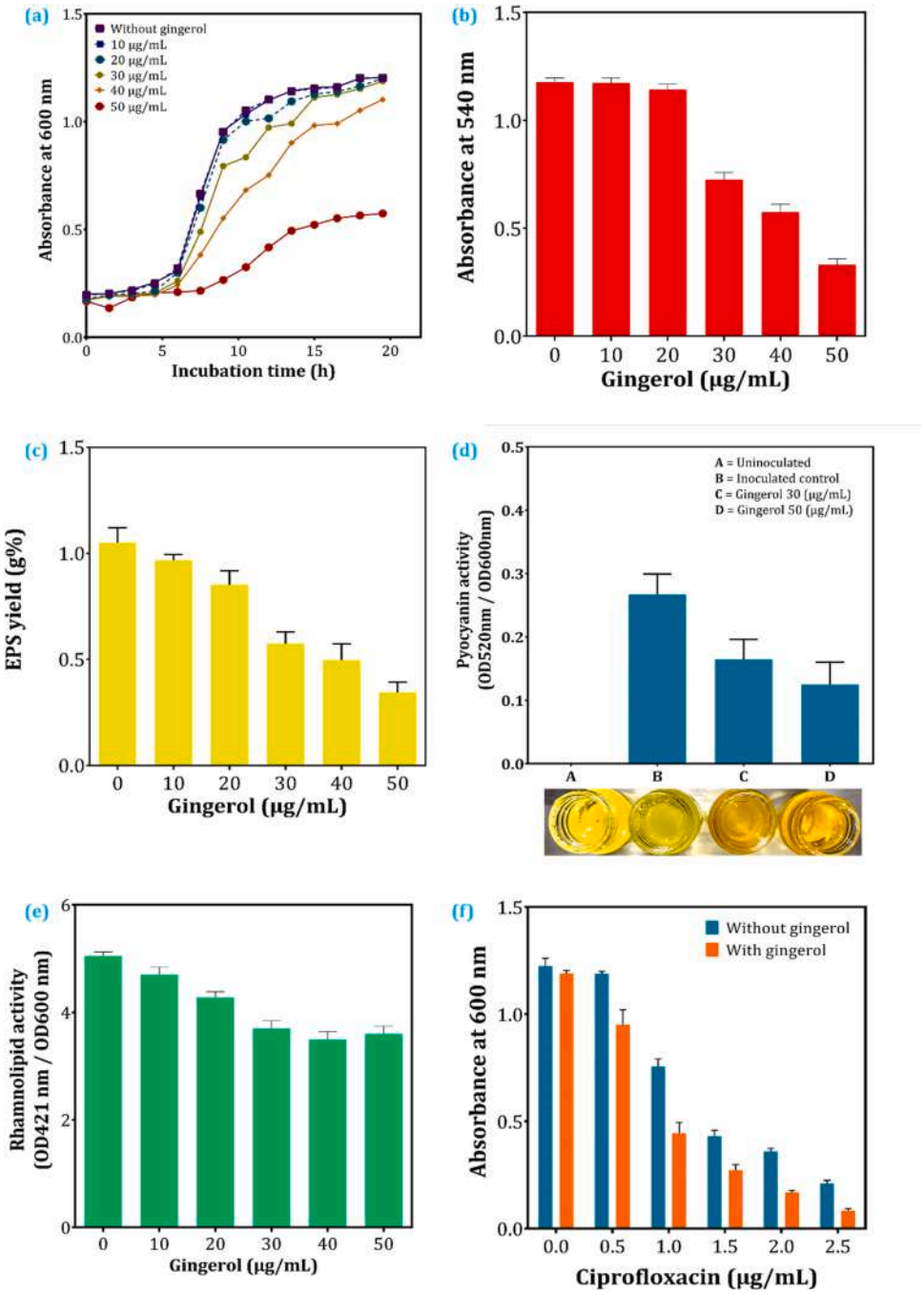

Fig. 6. (a) growth assessment of P. aeruginosa in presence of gingerol; assessing the impact of gingerol on (b) biofilm, (c) EPS, (d) pyocyanin, (e) rhamnolipid and (f) antibiotic susceptibility on *P. aeruginosa.*

molecular dynamics. The suppression effect of gingerol was found to be 100 µM (Kim et al., 2015) which we corroborated with our results showing similar impact with 30 µg/mL, normalizing these two values will yield same concentrations.

Moreover, there are several reports proving ginger to possess antibacterial properties at high concentration while at lower concentrations it tends to supress the physiological traits without reducing growth (Neyestani et al., 2019). From all the studies so performed, it can be inferred that (i) all three AHL receptors, LasR, PhzR and RhlR share striking structural similarity despite being poor in sequence similarity, (ii) gingerol tends to bind at the same binding cleft to that of native ligands of all these receptors however, as gingerol tends to make different sets of hydrophilic and hydrophobic interactions may distort the structural conformation of the protein which can inhibit its activity (iii) to prove this inhibition to have occurred, gingerol's negative influence in the production of biofilm, EPS, pyocyanin and rhamnolipid was observed which were all QS-driven (iv) as QS inhibition is proposed to weaken the survival traits of the bacteria, its impact on susceptibility towards antibiotic (ciprofloxacin) was studied and was found that in presence of gingerol, the effectiveness of antibiotic to control the growth of *P. aeruginosa* was observed. In summary, it can be concluded that the spontaneous binding of gingerol with various AHL receptors in *P. aeruginosa* inhibits various QS pathways weakening its armoury thereby making it more susceptible to antibiotic. In a nutshell, the authors conclude spontaneous binding of anti-QS gingerol with AHL receptors which may alter their conformation thereby thwarting their

appropriate function.

Author contributions

A.S. and D.G. conceived and designed the experiments; A.S. and P.P. performed the experiments; A.S. and D.G. analysed the data and wrote the manuscript; P.P. prepared figures for the manuscript whereas B.P. and M.S. reviewed the manuscript and provided necessary corrections.

Funding sources

This research did not receive any specific grant from funding agencies in the public, commercial, or not-for-profit sectors.

Declaration of Competing Interest

There is no conflict of interest.

Acknowledgements

The authors wish to thank Shri Dharamshi Solanki and Dr. Dharmesh Jaiswal from DST-FIST Sponsored Department of Microbiology & Biotechnology, Gujarat University (Ahmedabad, INDIA) for their untiring help in providing the necessary materials for the study.

Appendix A. Supplementary data

Supplementary material related to this article can be found, in the online version, at doi:https://doi.org/10.1016/j.micres.2021.126863.

References

Ahmed, S.A., et al., 2019. Natural quorum sensing inhibitors effectively downregulate gene expression of Pseudomonas aeruginosa virulence factors. J. Appl. Microbial. 103 (8), 3521–3535.
Ali, F., et al., 2018. In-silico prediction and modeling of the quorum sensing LuxS protein and inhibition of AI-2 biosynthesis in Aeromonas hydrophila. Molecules 23 (10), 2627.
Bekker, H., et al., 1993. Gromacs: a Parallel Computer for Molecular Dynamics Simulations.
Benkert, P., Biasini, M., Schwede, T., 2011. Toward the estimation of the absolute quality of individual protein structure models. Bioinformatics 27 (3), 343–350.
Berendsen, H.J., et al., 1981. Interaction models for water in relation to protein hydration. Intermolecular Forces. Springer, pp. 331–342.
Colovos, C., Yeates, T.O., 1993. Verification of protein structures: patterns of nonbonded atomic interactions. Protein Sci. 2 (9), 1511–1519.
Gasteiger, J., Jochum, C., 1979. An algorithm for the perception of synthetically important rings. J. Chem. Inf. 19 (1), 43–48.
Goswami, D., et al., 2015. Elucidating multifaceted urease producing marine Pseudomonas aeruginosa BG as a cogent PGPR and bio-control agent. Plant Growth Regul. 75 (1), 253–263.
Goswami, D., Thakker, J.N., Dhandhukia, P., 2016. Portraying mechanics of plant growth promoting rhizobacteria (PGPR): a review. J. Cogent Food Agric. 2 (1), 1127500.
Ham, S.-Y., et al., 2019. Control of membrane biofouling by 6-gingerol analogs: quorum sensing inhibition. J. Fuel 250, 79–87.
Hess, B., et al., 1997. LINCS: a linear constraint solver for molecular simulations. J. Comput. Chem. 18 (12), 1463–1472.
Kalia, V.C., et al., 2019. Quorum sensing inhibitors as antipathogens: biotechnological applications. J. Biotechnol. Adv. 37 (1), 68–90.
Kim, H.S., et al., 2015. 6-Gingerol reduces Pseudomonas aeruginosa biofilm formation and virulence via quorum sensing inhibition. Sci. Rep. 5, 8656.
Koh, C.-L., et al., 2013. Plant-derived natural products as sources of anti-quorum sensing compounds. J. Sens. 13 (5), 6217–6228.
Krivov, G.G., Shapovalov, M.V., Dunbrack Jr., R.L., 2009. Improved prediction of protein side-chain conformations with SCWRL4. Proteins 77 (4), 778–795.
Lee, J., Zhang, L., 2015. The hierarchy quorum sensing network in Pseudomonas aeruginosa. Protein Cell 6 (1), 26–41.
Li, X.H., Lee, J.H., 2019. Quorum sensing-dependent post-secretional activation of extracellular proteases in Pseudomonas aeruginosa. J. Biol. Chem. 294 (51), 19635–19644.
Marini, E., et al., 2015. Antimicrobial and anti-virulence activity of capsaicin against erythromycin-resistant. Cell-Invasive Group A Streptococci. 6 (1281).
Nasser, W., Reverchon, S., 2007. New insights into the regulatory mechanisms of the LuxR family of quorum sensing regulators. Anal. Bioanal. Chem. 387 (2), 381–390.
Nazzaro, F., Fratianni, F., Coppola, R., 2013. Quorum sensing and phytochemicals. Int. J. Mol. Sci. 14 (6), 12607–12619.
Nelson, D.L., Lehninger, A.L., Cox, M.M., 2008. Lehninger Principles of Biochemistry. Macmillan.
Neyestani, Z., et al., 2019. Review of anti-bacterial activities of curcumin against Pseudomonas aeruginosa. Crit. Rev. Eukaryot. Gene Expr. 29 (5).
O'Toole, G.A.J.J., 2011. Microtiter dish biofilm formation assay. Microtiter Dish Biofilm Formation Assay 47, e2437.
Parmar, P., et al., 2020. The Rise of Gingerol As Anti-QS Molecule: Darkest Episode in the LuxR-Mediated Bioluminescence Saga, p. 103823.
Pettersen, E.F., et al., 2004. UCSF Chimera—a visualization system for exploratory research and analysis. J. Comput. Chem. 25 (13), 1605–1612.
Pires, D.E., Blundell, T.L., Ascher, D.B., 2015. pkCSM: predicting small-molecule pharmacokinetic and toxicity properties using graph-based signatures. J. Med. Chem. 58 (9), 4066–4072.
Pronk, S., et al., 2013. GROMACS 4.5: a high-throughput and highly parallel open source molecular simulation toolkit. Bioinformatics 29 (7), 845–854.
Rao, P., et al., 2020. Reckoning a fungal metabolite, Pyranonigrin A as a potential Main protease (Mpro) inhibitor of novel SARS-CoV-2 virus identified using docking and molecular dynamics simulation. Biophys. Chem. 106425.
Rasmussen, T.B., et al., 2005. Screening for quorum-sensing inhibitors (QSI) by use of a novel genetic system, the QSI selector. J. Bacteriol. 187 (5), 1799–1814.
Shukla, A., et al., 2019. Depicting the Exemplary Knowledge of Microbial Exopolysaccharides in a Nutshell.
Shukla, A., et al., 2020. Twin peaks: presenting the antagonistic molecular interplay of curcumin with LasR and LuxR quorum sensing pathways. Curr. Microbiol.
Szabó, M.Á., et al., 2010. Inhibition of quorum-sensing signals by essential oils. J. Phytother. Res. 24 (5), 782–786.
Trott, O., Olson, A.J., 2010. AutoDock Vina: improving the speed and accuracy of docking with a new scoring function, efficient optimization, and multithreading. J. Comput. Chem. 31 (2), 455–461.
Turner, P.J.C.f.C, O.G.I.o.S. Land-Margin Research, B. Technology, OR, 2005. XMGRACE. Version 5.1. 19..
Van Der Spoel, D., et al., 2005. GROMACS: fast, flexible, and free. J. Comput. Chem. 26 (16), 1701–1718.
Wang, J., et al., 2001. Antechamber: an accessory software package for molecular mechanical calculations. J. Am. Chem. Soc. 222, U403.
Zoete, V., et al., 2011. SwissParam: a fast force field generation tool for small organic molecules. J. Comput. Chem. 32 (11), 2359–2368.